MAGNET STRUCTURE AND INTEGRATION

TASK: Development of chemical deposition methods for the fabrication of YBCO high temperature superconducting coated conductors for high-field applications

<u>*Deliverable*</u>*: $Y_{1-x}Ca_xBa_2Cu_3O_y$ targets for pulsed laser deposition (PLD) of thin films and chemically CeO_2 buffered biaxially textured Ni-W substrates for the development of high temperature superconducting coated conductors*

Traian Petrisor, Lelia Ciontea

Technical University of Cluj-Napoca, Cluj-Napoca

1. <u>Ca-doped YBCO targets for the manufacturing of $Y_{1-x}Ca_xBa_2Cu_3O_y$ thin films by PLD</u>

1.1 Manufacturing of $Y_{1-x}Ca_xBa_2Cu_3O_{7-y}$ targets for laser ablation

Samples of the composition $Y_{1-x}Ca_xBa_2Cu_3O_{7-y}$ with x=0, 0.05, 0.07, and 0.10 were prepared by solid state reaction from Y_2O_3 (99,99%), $CaCO_3$ (99.9 %), $BaCO_3$(99.9%), CuO (99,9%). Appropriate amounts of Y_2O_3, $CaCO_3$, $BaCO_3$ and CuO were manual ground and heated in air at 950°C for 24 hours in alumina crucibles. The samples were reground and pressed at 300 MPa into pellets of 30 mm in diameter and sintered at 950°C for 8 hours in flowing oxygen atmosphere.

It was established by thermogravimetry that in these materials the oxygen has a very high diffusion rate at about 450°C. It was also established that the oxygen amount is inversely proportional with the cooling rate. Taking into account these observations, the samples were both slowly cooled and annealed at 500°C for 6h in flowing oxygen atmosphere. We used the same rate (2°C/min) for cooling from 950-500°C and from 500°C to room temperature.

1.2 Film processing and results

The films were grown on $SrTiO_3$ (100) substrates by means of PLD from a sintered $Y_{1-x}Ca_xBa_2Cu_3O_{7-\delta}$ target, in a pure O_2 atmosphere. The substrate temperature was 850 ˚C and the oxygen pressure 40 Pa. The oxygenation process takes place at 450 ˚C in 75 kPa of oxygen for 10 minutes. More details on the deposition process were published elsewhere [1]. The structural properties of the films have been studied by X-ray diffraction (XRD); the films resulted c-axis oriented with <u>F</u>ull <u>W</u>idth <u>H</u>alf <u>M</u>aximum of the ω-scan around the (005) peak

of about 0.3°. The samples have then been processed by the usual UV photolithography and ion beam etching to obtain 2 mm long strips, 30 µm or 50 µm wide. The film thickness d, measured by a stylus profilometer, is $d \approx 220$ nm. The contact pads were first cleaned by argon etching and then covered by a 0.5 µm thick silver layer deposited above and patterned by using the lift-off technique. The samples were then put on a sample holder and loaded into a He gas flow cryostat provided with a superconducting magnet. In this condition the applied magnetic field H was parallel to the c axis of the films and perpendicular both to the bias current and to the film surface. We set the critical current density value with the usual 1µV/cm electric field E criterion.

In Figure 1 the zero resistance critical temperature T_c of the unpatterned films as a function of the Ca doping amount in the YBCO target is reported. As expected, T_c is a decreasing function of the Ca concentration in agreement with the results obtained by others [2,3]. However, a spread of T_c for the same amount of Ca concentration has been found, thus not allowing to remark differences between the 5% and 7% Ca doping.
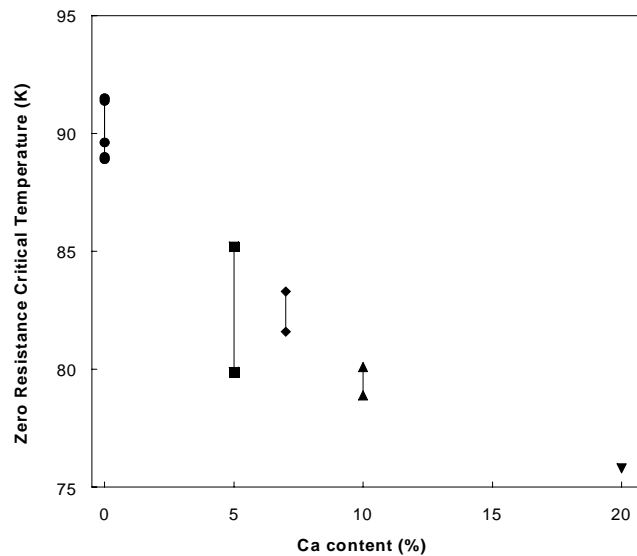

Figure 1. T_c of the $Y_{1-x}Ca_xBa_2Cu_3O_{7-\delta}$ films as a function of the nominal target Ca concentration.

Figure 2 shows the resistive transition $\rho(T)$ of the $Y_{1-x}Ca_xBa_2Cu_3O_{7-\delta}$ patterned samples. The resistivity values at room temperature lie between 1.8 and 3.0×10^{-6} Ω.m at 300 K. The normal state resistivity seems to be related to the Ca content, increasing with doping. The resistivity of the undoped sample does not scale as expected. However, previous studies on the resistivity dependence on the Ca doping is quite contrasting indicating a not clear trend. The inset shows the magnified transition region. It has to be noted that the Ca 5% T_c is slightly below the T_c of the Ca 7% sample.

The T_c dependence on oxygen annealing pressure was also studied. The results obtained for 1 hour of annealing at different oxygen pressures is reported in Figure 3. The samples with Ca exhibit the maximum T_c (83.4 K and 82.5 K for 10% and 20%, respectively) for annealing oxygen pressure in the range (0.3-1) Torr, but in 20% Ca substituted YBCO films the T_c decrease is steeper out of this range.

The T_c can be related to the concentration of holes, p, using the approximated parabolic formula [4]:

$$\frac{T_c}{T_c^*} = 1 - 82.6\left(p - p^*\right)^2 \qquad (1)$$

where T_c^* is the maximum critical temperature and p^* is the corresponding optimal carrier concentration, which is generally considered as 0.167 holes per CuO plane for the $Y_{1-x}Ca_xBa_2Cu_3O_{7-\delta}$ systems.
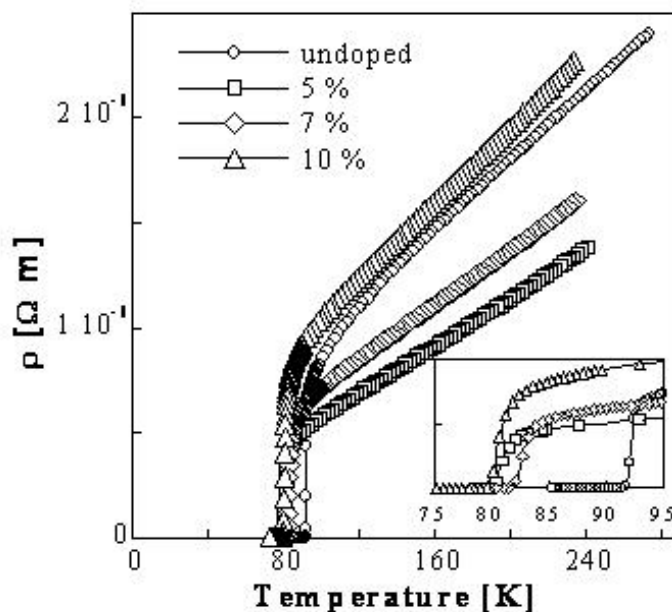

Figure 2. Resistive transition of the $Y_{1-x}Ca_xBa_2Cu_3O_{7-\delta}$ stripe lines. In the inset the transition region is magnified.
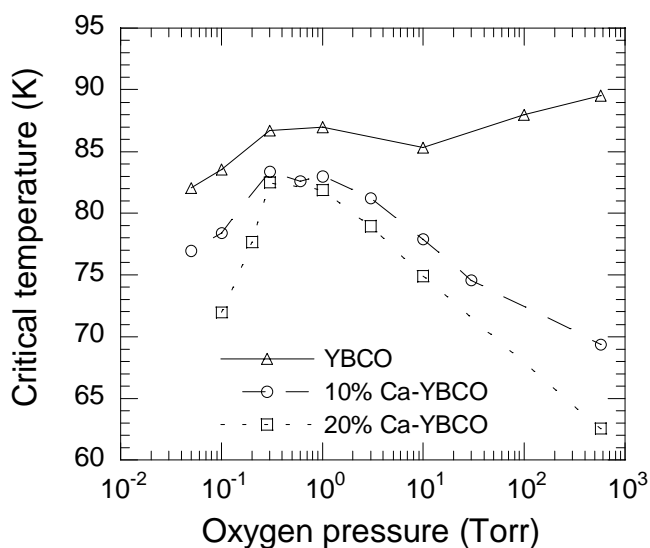

Figure 3. T_c versus annealing pressure for all the three Ca concentrations studied. Annealing time was 1 hour. The lines are guides for the eye.

In Figure 4, the J_c-vs-B behavior is shown for different Ca doped films at 77 K. The undoped sample shows the best performance, while the Ca content generally decreases J_c. This can be ascribed to the different reduced temperature $t=T/T_c$, where the value increases for the doped samples. Considering the J_c-vs-B curves at the same t, the transport properties become more similar to the undoped sample. At $t = 0.865$, corresponding to 77 K for YBCO, the dependences overlap.
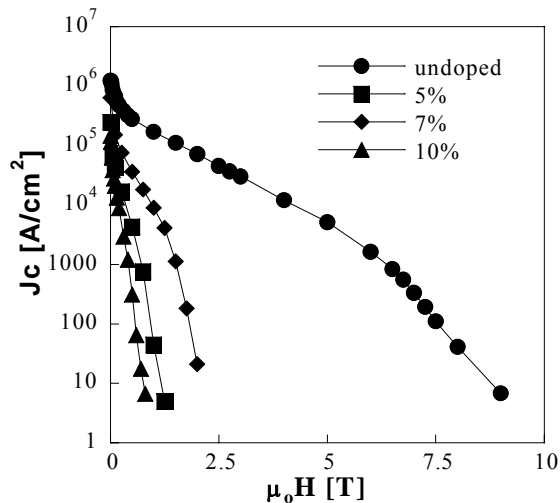

Figure 4. Jc(B) for different Ca doped films recorded at 77 K.

2. <u>Ni-W biaxially textured substrates chemically buffered with CeO$_2$</u>.

2.1 Experimental details

The Ni-5at.%W solid solution was prepared from 99.95+% pure Ni and W in an argon-arc furnace with water-cooled copper hearth. The {100}<100> cube textured Ni-W substrates with a thickness of about 100 μm were obtained in a conventional way, by a cold-rolling process followed by a recrystallization heat treatment. The relative reduction in thickness $[\rho=(t_0-t)/t_0]$ and the corresponding true strain $[\varepsilon=\ln t_0/t]$ were 97% and 2.5, respectively. During the rolling process the deformation step was continuously decreased to maintain the plain strain deformation [5]. Finally, the primary recrystallization annealing was performed in vacuum (10^{-7} Torr) at 900 °C for 4 hours.

The coating solution has been prepared [6, 7, 8] by two methods, as follows:

a) First, by charging a flask with 1 g of cerium isopropoxide 97%(AlfaAesar) and 25ml of 2-methoxyethanol (AlfaAesar). The content of the flask was refluxed for 1 hour and 15ml of solvent (a mixture of isopropanol and 2-methoxyethanol) was removed by distillation. The content was rediluted with 25 ml additional 2-methoxyethanol and the distillation/redilution cycle was repeated several times to ensure the exchange of the isopropoxide ligand for the methoxyethoxide ligand in as much as possible. Due to the intrinsic insolubility of cerium isopropoxide in 2-methoxyethanol, a supplementary filtration was necessary to remove the unreacted solid. The final concentration was adjusted to about 0.15 molar. Difficulties have

been also encountered in the preparation in house of cerium isoproxide from cerium metal and isopropanol in the presence of a mercury salt catalyst by the method described by Brown and Mazidiyansi. The reaction is slow and hard to drive to completion.

b) Second, diluting the as purchased 18-20 % wt. cerium (IV) methoxyethoxide in a 2-methoxyethanol (AlfaAesar) solution was brought to a concentration of 0.25 molar. For the partial hydrolysis, four parts of the as-obtained solution were mixed with one part 1.0 molar H_2O in 2- methoxyethanol to produce the coating solution.

2.2 Structural and morphological properties of CeO₂ buffer layer

Figure 5 shows a typical θ-2θ scan for a 300 nm thick CeO₂ film deposited on a biaxially textured Ni-W substrate. The strong CeO₂ (200) and (400) peaks are consistent with a good epitaxially CeO₂ film grown with the [100] direction perpendicular to the substrate. Moreover, the (111) to (200) intensity ratio is less than 0.3%, indicating a small volume percentage of (111) oriented grains. The X-ray ω-scans reveal a good out-of-plane oriented film. The full width at half maximum (FWHM) of the ω-scans for CeO₂ (200) peak, measured in the rolling direction (RD), is of about 3.5°. In-plane alignment of the CeO₂ film was measured by means of the pole figures. A single CeO₂[100]//Ni-W[110] epitaxial orientation of the CeO₂ layer is evident. The FWHM of the ϕ -scan for CeO₂(111) peak was 6.5°.
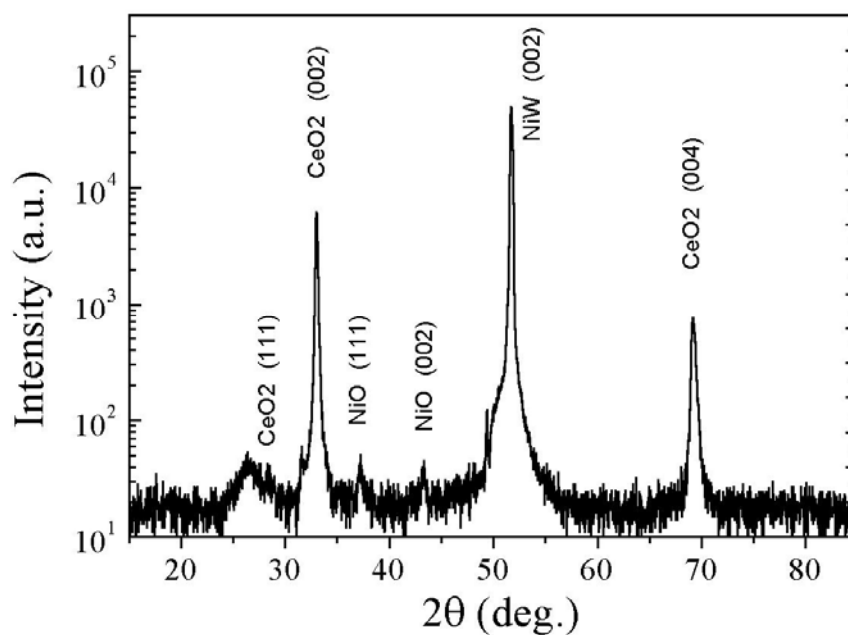

Figure 5.   X-ray θ-2θ diffraction pattern of CeO₂ 500 nm thick buffer layer on Ni₉₅W₅ biaxial textured substrate

SEM studies of the CeO₂ film revealed a uniform, smooth and crack-free CeO₂ surface as can be observed from Figures 6a and b. The film exhibits a smooth and crack-free surface (Figure 6b). The cross-section SEM studies have shown that the films have dense microstructures, without cracks or porosity. Moreover, the as deposited film exhibits a uniform microstructure over the substrate grain boundary, indicating a good coalescence of the CeO₂

film grown on the Ni-W substrates. This has a positive influence on the transport properties of the subsequently deposited YBCO film. The CeO_2-Ni-W interface is smooth and is a replica of the substrate morphology. Taking into account these observations and the structural analyses, one can conclude that the oxidation resistance of the Ni-W substrate is high enough to permit a good epitaxial deposition of CeO_2 .

a   b
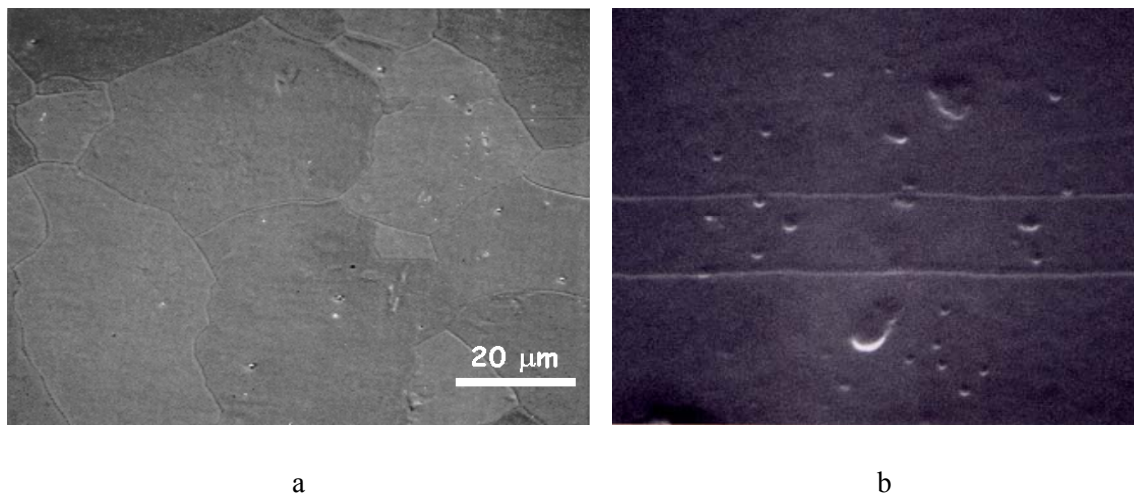
Figure 6. SEM micrograph of the CeO_2 film on the Ni-W substrate. Low magnification (a) and high magnification (b), respectively.

Conclusions:

In summary, transport measurements on epitaxial superconducting $Y_{1-x}Ca_xBa_2Cu_3O_{7-y}$ thin films deposited on $SrTiO_3$ single crystal substrates by the PLD technique have been performed. It was observed that the critical temperature decreases with increased Ca doping, as expected. In spite of the lower critical temperature, the Jc values of doped samples in applied magnetic field have reached the same values for YBCO at a reduced temperature of about 0.865. The study of the transport properties at different applied magnetic fields revealed a shift of the irreversibility line of about 9 K at 1 and 3 T comparing the undoped YBCO with the 5% Ca doped sample.This study has revealed that a sharp cube texture can be easily developed in Ni5at%W with the FWHM of the out-of-plane and in-plane textures of 5.6° and 7°, respectively. Moreover, the fraction of misoriented and twinned grains is more reduced for the Ni-W with respect to other Ni-based substrates (e.g. Ni11at %V and Ni12at %Cr) and, as a consequence, the Ni-W substrate has a smoother surface, which is very important for obtaining high J_c coated conductors. Due to the high oxidation resistance, the Ni-W substrate permits the epitaxial deposition of CeO_2 oxide buffer layer by chemical methods. This is of a great interest for the fabrication of long lengths of high J_c tapes for the power applications.

Publications:

Augieri A., Petrisor T., Celentano G., Ciontea L., Galluzzi V., Gambardella U., Mancini A., Rufoloni A., *"Effect of Ca doping in YBCO Superconducting Thin Films"*, Physica C 401 (2004), 320-324.

Cancellieri C., Augieri A., Boffa V., Celentano G., Ciontea L., Fabbri F., Galluzzi V., Gambardella U., Grassano G., Petrisor T., Tebano R., *"Deposition and characterization of $Y_{1-x}Ca_xBa_2Cu_3O_{7-\delta}$ epitaxial thin films"*, presented at ASC04, accepted for publication in IEEE Transactions on Applied Superconductivity.

References:

[1] **Fabbri F., Padeletti G., Petrisor T., Celentano G., Boffa V.**,

Supercond. Sci. Technol. 13, 1492 (2000)

[2] **Bandyopadhyay S. K., et al.**, Phys. Lett. A 226, 237 (1997)

[3] **Bernhard C., Tallon J. L.**, Phys. Rev. B 54, 10201 (1996)

[4] **Presland M. R., Tallon J. L., Buckley R. G., Liu R. S. and Flower N. E.**, *"General trends in oxygen stoichiometry effects on T_c in Bi and Tl superconductors"*, Physica C, vol. 176, 95, 1991.

[5] **Mao W.,** Mat. Sci. Eng., A257 (1998) 171

[6] **Akin Y., Celik E., Sigmund W. and Hascicek Y. S.**,

IEEE Transactions on Applied Superconductivity, vol.13 (2003) 2563.

[7] **Akin Y., Aslanoglu Z., Celik E., Arda L., Sigmund W. and Hascicek Y. S.**, IEEE Transactions on Applied Superconductivity, vol.13 (2003) 2673.

[8] **Goyal A., Feenstra R., Paranthaman M., Thomson J. R., Kang B. Y., Cantoni C., Lee D. F., List F. A., Martin P. M., Lara-Curzio E., Stevens C., Kroeger D. M., Kowalewski M., Specht E. D., Aytung T., Sathyamurthy S., Williams R. K., Ericson R. E.,**, Physica C 382 (2002) 251.